Automated Water Spread Mapping Using ResourceSat-1 AWiFS Data for Water Bodies Information System

S. Subramaniam, A. V. Suresh Babu, and Partha Sarathi Roy

***Abstract*—Water resources planning and management requires data collection, analysis and monitoring of critical parameters like spatio-temporal water spread information and expected volumes. Temporal fluctuations in water resources can be studied through frequent spatial inventory of surface water bodies. Application of geospatial information technologies, namely Satellite Remote Sensing and Geographical information Systems (GIS), offer immense scope for replacing/supplementing the traditional monitoring methods. The traditional classification algorithms, namely supervised, unsupervised, band thresholds, Normalized Difference Water Index (NDWI) and Modified Normalized Difference Water Index (MNDWI), require a decision-based approach for each scene, which is highly subjective. Hence, suitable automatic extraction methods need to be developed. A new knowledge-based algorithm has been developed using multi-temporal spectral information available in four bands of Advanced Wide Field Sensor (AWiFS) on board ResourceSat-1 (with spatial resolution of 56 m) namely Green (G), Red (R), Near Infrared (NIR) and Short Wave Infrared (SWIR) for inventorying and monitoring of various types water bodies. The algorithm has been applied for the data obtained from other space-borne sensors with similar spectral bands such as Landsat ETM, IRS LISS III and ASTER and found to be working satisfactorily. Results were validated by comparing the results reported from other popular methods. The study provides a quick method for generation of spatio-temporal water bodies information. This will be helpful for development of Water bodies Information System (WIS) on national/global scales.**

***Index Terms*—Automation, remote sensing.**

I. Introduction

SUSTAINABILITY of water resources is one of the critical factors in maintaining human civilization as it exists today. But with the current trend in modifications in the land cover of the world, more so in the populated developing countries, the long-term sustainability of water resources is a question. Mapping and regular monitoring of surface water bodies for the availability of water resources at river basins/sub basins, regional, state and country level is an important aspect of water resources planning and management in India. Conventionally, water resources management has been carried out in the country using the gauges maintained at all the major/medium reservoirs and in river reaches. Satellite remote sensing data provide a synoptic coverage of fairly large areas at frequent intervals, enabling thereby to monitor the water bodies and capture their geospatial and temporal variability of water spreads; thus helping in the assessment of inter/intra-annual variations in water spread. The availability of medium spatial resolution data from Advanced Wide Field Sensor (AWiFS) onboard ResourceSat-1 with 56 m spatial resolution; 5 days repetivity and 740 km swath has enabled the prospects of near-real-time monitoring of water bodies. Using IRS AWiFS data, spatio-temporal information on water bodies has been generated by developing automatic feature extraction algorithm. The algorithm enables quick processing of data and dissemination of water spread information through a web-enabled information system useful for water resources planners/managers.

AWiFS sensor provides data in four spectral bands, namely Green, Red, Near Infrared (NIR) and Short Wave Infrared (SWIR) regions of electromagnetic spectrum. Distinct spectral reflectance characteristics of water in the above four bands compared to other non-water features has led to the automatic extraction of water bodies. To date, numerous classification techniques for the extraction of water bodies from satellite data have been reported based on the spectral separability of the water bodies in the visible and infrared regions of the spectrum [1], [2]. Frazier *et al.* [3] have used Landsat TM data for mapping riverine water bodies. Manavalan *et al.* [4] have used water spread areas derived from multi-temporal satellite images to estimate live storage capacity of the reservoirs. Suresh Babu *et al.* [5] have estimated the water spread area of the Tungabhadra reservoir, India, and estimated the volume of water that has been stored between various reservoir operating levels using IRS AWiFS data. Sagar *et al.* [6] have worked on the distribution of water bodies using satellite data analysis. ResourceSat-1 AWiFS sensor data was used for developing an algorithm to monitor the snow cover for the Himalayan region at fortnightly intervals by Kulkarni *et al.* [7]. Suresh Babu *et al.* [8] have defined the concept of automatic extraction of water bodies from satellite data. The present study aims at automated water spread mapping which encompasses spectral characterization of various types of water bodies and development of

Manuscript received May 17, 2009; revised October 23, 2009, January 29, 2010, and May 27, 2010; accepted September 09, 2010. Date of publication October 21, 2010; date of current version March 23, 2011.

S. Subramaniam and A. V. Suresh Babu are with the RS & GIS Applications Area, National Remote Sensing Centre (NRSC), Indian Space Research Organisation (ISRO), Department of Space, Govt. of India, Hyderabad, AP, 500 625 India (e-mail: avsureshbabuisro@gmail.com).

P. S. Roy is with the Indian Institute of Remote Sensing (IIRS), National Remote Sensing Centre (NRSC), Indian Space Research Organisation (ISRO), Department of Space, Govt. of India, Dehradun, Uttarkhand, 248 001 India.

Color versions of one or more of the figures in this paper are available online at http://ieeexplore.ieee.org.

Digital Object Identifier 10.1109/JSTARS.2010.2085032

spectral relationships and algorithm for the extraction of water features that facilitates quick processing.

II. Need for the Development of New Automated Algorithm

Information on the water spread and extent have been generally extracted from space-borne multi-spectral digital images using supervised/unsupervised classification techniques. Most of the contemporary image processing software, *viz.* ERDAS imagine, ENVI, Geomatica, ILWIS, etc., have these modules. These methods involve the extraction of inherent spectral patterns in the satellite data and require further interpretation to group certain classes to derive information on water spread. For example, in supervised classification, training set signatures from various types of water bodies in a particular image are the basis for the classification which may not accommodate all types of water bodies that might exist in other images across the region. Similarly, in unsupervised classification, number of classes are defined and classified. The corresponding classes pertaining water pixels have to be determined by visual interpretation techniques by the analyst to arrive at water layer. In the band thresholding method, digital number (DN) threshold ranges for a water pixel in different bands are defined and are used for extraction of water bodies. These methods are however scene specific, and thus may not be applicable to other areas.

Spectral response patterns of water, vegetation and soil measured from field spectrometer are shown in Fig. 1(a), and Fig. 1(b) indicates the contrast between spectral reflectance of water in the visible and infrared regions of the electromagnetic spectrum and the rest. The high contrast in the reflectance of water in green spectral range with respect to the NIR and SWIR region is an important characteristic. These characteristics were used to automatically delineate water feature using Normalized Difference Water Index (NDWI) [9]. The NDWI was subsequently refined as the Modified Normalized Difference Water Index (MNDWI) [10]. The definitions of these spectral indexes are

$$\mathrm{NDWI} = \frac{\mathrm{Green} - \mathrm{NIR}}{\mathrm{Green} + \mathrm{NIR}} \tag{1}$$

$$\mathrm{MNDWI} = \frac{\mathrm{Green} - \mathrm{SWIR}}{\mathrm{Green} + \mathrm{SWIR}} \tag{2}$$

where Green represents the reflectance of the green band (band 2 of AWiFS), NIR represents the reflectance of the near infrared band (band 4 of AWiFS), and SWIR represents the reflectance of the short wave infrared band (band 5 of AWiFS).

The implementation of spectral indexes like NDWI and MNDWI requires selection of suitable threshold limits for identification of pixels corresponding to water. The threshold limits are highly subjective and vary from image to image and across the time periods, even within a image, thereby leading to the introduction of error in the output. Further, these indexes are also dependant on the spectral information available in only two spectral bands and spectral information available in other bands has not been utilized. Further, these indexes are not effective in the case of noise features like cloud, cloud shadow and urban areas. Utilization of all the bands in combination may help in delineating water bodies in cloud-infested areas or urban agglomerations. Hence, there is a need for the development of a new algorithm that utilizes the information from all the spectral bands to eliminate the noise feature while extracting water feature.

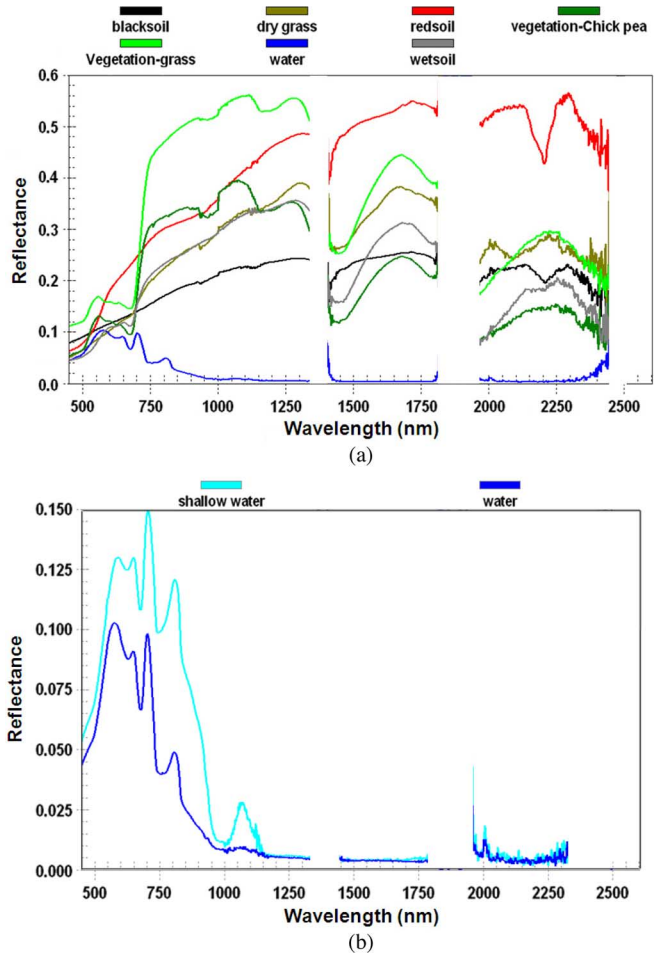

Fig. 1. Spectral reflectance characteristics of various land cover features and water. (a) Various Landcover features; (b) water features.

III. Development of Algorithm for Automatic Water Bodies Extraction

The development of the algorithm in the present study involves extraction of sample pixels data of various types of water bodies from IRS AWiFS sensor data in different seasons and analysis of spectral characteristics. It also involves development of spectral relationships and formulation of logics. The specifications of AWiFS sensor of ResourceSat-1 [11] are given in Table I.

Spectral response pattern of water bodies presented in Fig. 1 corresponds to *in situ* measurements. However, in the case of air or space-borne measurements, the spectral response pattern is modified due to atmospheric constituents, variations of sun's illumination geometry, and sensors, etc. It may introduce noise/error in the classification of water bodies. The conversion of image DN values to Top Of the Atmosphere (TOA) reflectance value [12] has been advocated to account for illumination of sensor geometry except for the atmospheric effect. We have,

TABLE I
SPECIFICATIONS OF IRS AWiFS SENSORS

S.No	Parameter	Value			
1	Ground sampling distance (m) Across track Along the track	 56 (nadir), 70 (off-nadir) 66 for integration time of 9.96msec			
2.	Swath (w/o earth curvature effect)	740 Km			
3	Bands (μm)	B2	B3	B4	B5
		0.52-0.59	0.62-0.68	0.77-0.86	1.55 -1.7
4	Quantization (Bits)	10			
5	Band to band registration (pixel)	≤±0.25			

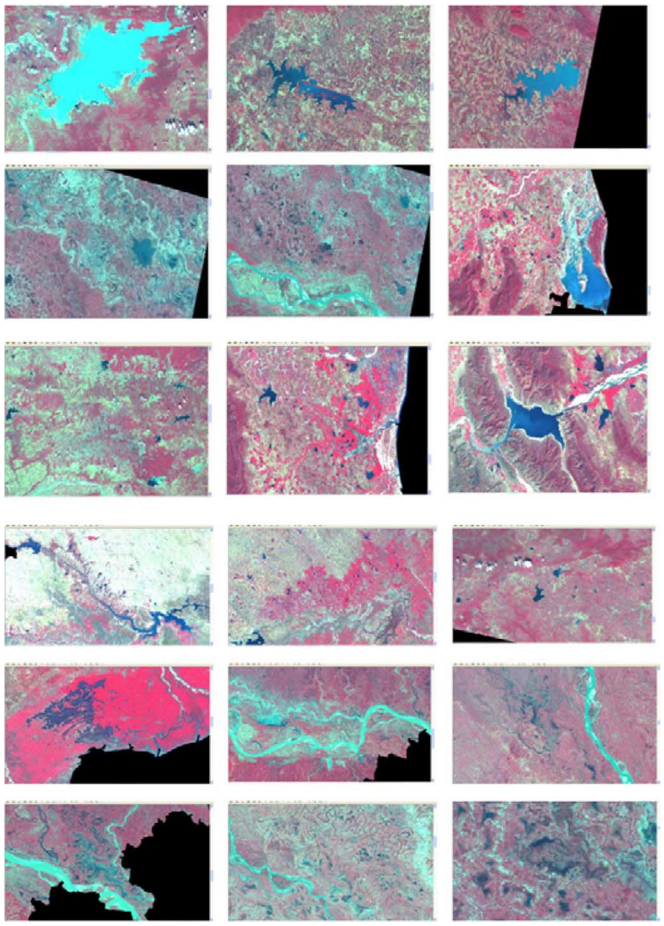

Fig. 2. Sample AWiFS images (containing water bodies) used in signature analysis.

therefore, TOA reflectance values for development of an algorithm for delineation of water bodies used in the study. The TOA reflectance (pTOA) is computed using the following equation:

$$\rho\mathrm{TOA} = (\pi\, \mathrm{L}\lambda\, \mathrm{d}^2)/(\mathrm{ESUN}\cos(\Theta\mathrm{s})) \tag{3}$$

where $\rho\mathrm{TOA}$ = TOA reflectance; $\mathrm{L}\lambda$ = spectral radiance at sensor aperture $(\mathrm{mWcm}^{-2}\mathrm{sr}^{-1}\mu^{-1})$; d = Earth–Sun distance (Astronomical Units); ESUN = mean solarexoatmospheric irradiance $(\mathrm{mWcm}^{-2}\mathrm{sr}^{-1}\mu^{-1})$; and $\Theta\mathrm{s}$ = solar zenith angle (degrees).

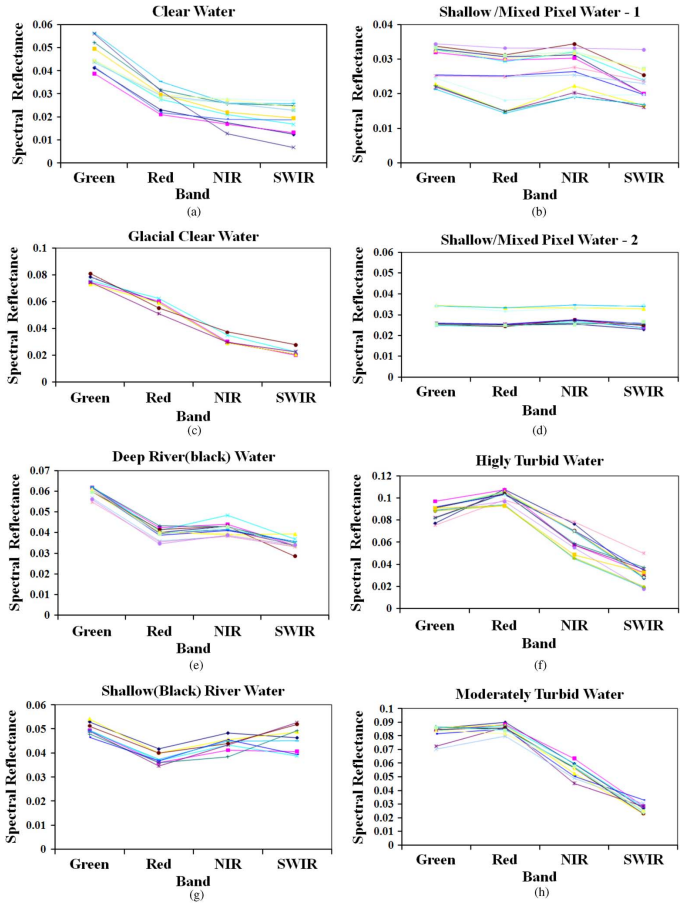

Fig. 3. TOA spectral reflectance pattern for different water types.

Spectral response analysis and characterization of various sub-categories of water were carried out using sample pixels extracted from various types of water bodies, namely clear water, water with different depths, turbidity levels, river water, and water under hazy cloud cover, selected from multi-seasonal/multi-year AWiFS data across India. Typical examples depicted across several types of water bodies are shown in Fig. 2.

Characterization of spectral response pattern of water bodies with varying depth, turbidity, shape, and size is essential for development of a knowledge-based, hierarchical algorithm. Also, the spectral characteristics of features like cloud, urban settlements, and cloud's shadow that introduces noise to the water body extraction also need to be studied. The typical spectral response pattern of various types of water bodies along with their variations is shown in Fig. 3. Important characteristics of water in the visible SWIR spectral bands are (i) lower reflectance in visible SWIR spectral region compared to other surface cover features due to the absorption of NIR and SWIR radiation; (ii) high spectral contrast between green and NIR/SWIR; and (iii) the reflectance of clear water in the NIR spectral band is lower in NIR as compared to red band, a negative value of NDVI estimation.

The feature extraction algorithm uses contrast between the feature of interest (water) and other features for the elimination of the pixels corresponding to other land cover types. It uses spectral variability within water for the identification of

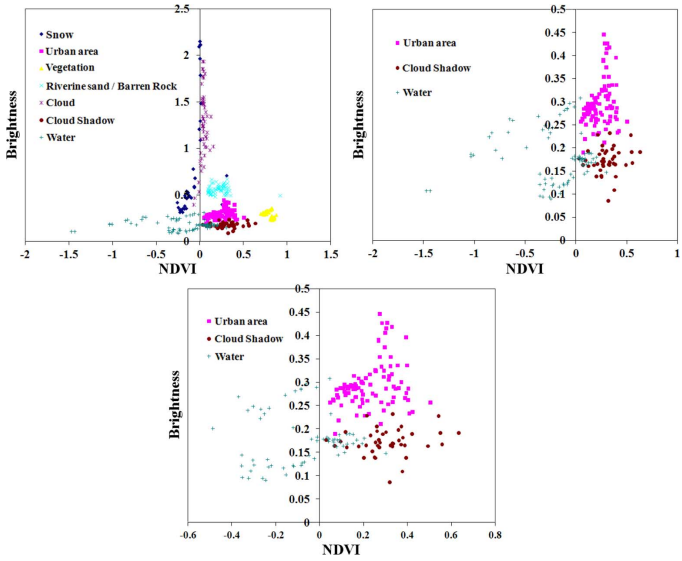

Fig. 4. Scatter plot of brightness for various land cover and noise features as a function of NDVI.

the water feature pixels. The same has been implemented in a hierarchical, logical sequential step for development of an automatic extraction algorithm. To arrive at the required hierarchical logical steps of the algorithm, various spectral parameters such as total brightness (sum of responses from four bands), NDWI, MNDWI, NDVI spectral ratios, etc., were computed from Green, Red, NIR and SWIR reflectance data. These spectral parameters were analyzed for identification for their discriminating characteristics of water from other land cover types and noise.

Many researchers have used the low reflectance of water bodies for their identification using the band threshold logic. Further, it is evident from Fig. 1 and Fig. 3(a) and (b) that the reflectance of water in the NIR spectral band is lower than that in the red band. The NDVI values of water computed from its spectral response in NIR and Red would have negative values. These two observations were used to remove non-water pixels during image analysis. Fig. 4 shows the scatter plot of various types of water body pixels, other land cover categories. A close look at the plot shows that most of the non-water pixels can be eliminated by setting the upper threshold limit of NDVI as 0.25 and the brightness value (sum of TOA reflectance values of all the bands) to 0.3. The higher threshold of NDVI is needed to account for the presence of aquatic vegetations and mixed water–land pixels having vegetation in the land portion.

From the spectral reflectance of turbid water [Fig. 3(g) and (h)], it can be inferred from these figures that the reflectance in Red and NIR spectral bands are more for turbid water compared to other water types. Since, the reflectance patterns are similar to that observed from *in situ* measurements [13], [14]. a higher threshold limit of 0.4 for the brightness has been used for identification of turbid water pixels.

From the spectral reflectance pattern of clouds and cloud shadows [Fig. 5(a) and (b)], it can be observed that few sample pixels have lower reflectance values in NIR and SWIR bands compared to the green band. This implies that these pixels would be also be categorized as water, if the standard indexes

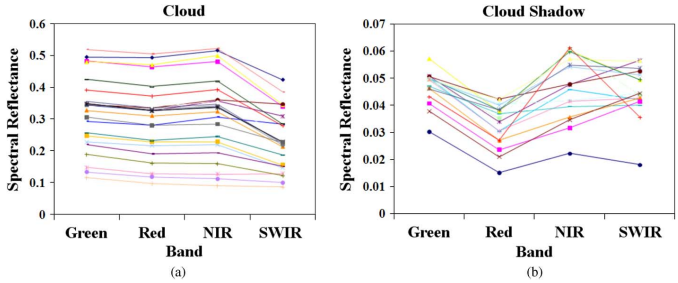

Fig. 5. Spectral reflectance pattern (TOA) of cloud and cloud shadow.

such as NDWI/MNDWI were used. Further, it is also clear from spectral plots of cloud that most of the cloud pixels have higher reflectance in all the bands and get eliminated by the brightness threshold limits. The cloud shadow has higher NDVI and therefore they are labeled as non-water pixels with the thresholds set for NDVI. The logic for the elimination of most of the non-water pixels is given below:

$$\begin{aligned}&\text{IF} \quad ((\text{NDVI} < 0.25)\ \text{AND}\ (\text{Brightness} < 0.3))\\ &\qquad \text{THEN}\ \{\text{probable water pixel}\}\\ &\text{ELSE} \quad \text{IF}\ ((\text{NDVI} < 0.25)\ \text{AND}\ (\text{Brightness} < 0.4))\\ &\qquad \text{THEN}\ \{\text{probable turbid water}\}\\ &\text{ELSE}\ \{\text{Non-Water pixel.}\}\end{aligned} \tag{4}$$

The reflectance of water pixels in the green band was found to be greater than that of the red band and the NIR/SWIR band or both (Fig. 3). This logic was utilized at the second level of hierarchy for detection of water pixels and implemented as given below:

$$\begin{aligned}&\text{IF}\ ((\text{B2} > \text{B3})\ \text{AND}\ ((\text{B2} > \text{B4})\ \text{OR}\ (\text{B2} > \text{B5})))\\ &\text{THEN}\ \{\text{Enter next level in water logic}\}\end{aligned} \tag{5}$$

The discriminating logics for different types of water pixels are implemented in the third levels of logical equations. The logical equation for each sub-category of water uses multiple logics with suitable threshold values for each of the selected parameters. The parameter sets used and their individual threshold values vary with water feature types. Detailed analysis of a large number of carefully selected pixels was carried out to arrive at the particular set of logics and the threshold values for each of the parameters.

The approach used for identification of a set of parameters for each of the sub-categories of water at the next level of hierarchical logic for NDWI and MNDWI based analysis is shown in Fig. 6 and Fig. 7. Similar plots with other spectral indexes and spectral band ratios were also analyzed and feature parameters that provide maximum discrimination for the water feature were selected.

The mean, standard deviation, maximum and minimum values of the parameters were computed and compared with those of noise feature (cloud/cloud shadows) values to arrive at the threshold values for each of the selected parameters. Fig. 8 shows the scatter plot of the selected parameters in the case of clear water. The clear water pixels can be discriminated by setting these ratios greater than 1.0 [Fig. 1, Fig. 3(a) and (b)].

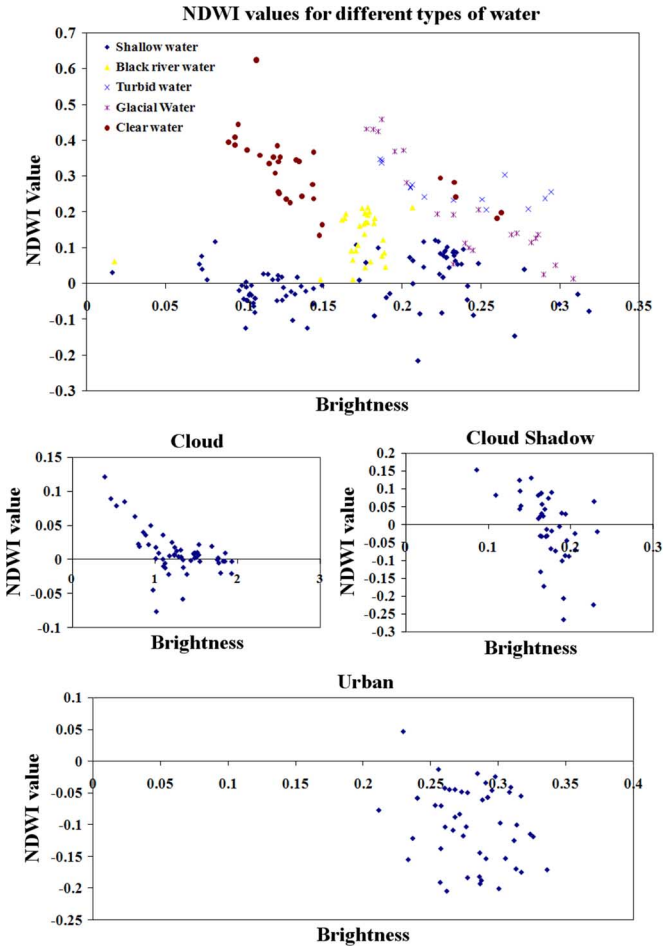

Fig. 6. Scatter plots showing NDWI values as a function of brightness for various types of water and noise features.

The logical implementation for clear water pixels takes the form:

$$\text{IF } ((\text{B3} > \text{B4}) \text{ AND } (\text{B2} > \text{B5})) \text{ THEN } \{\text{clear water}\} \text{ ELSE } \{\text{Check for other types of water}\}. \quad (6)$$

Mixed water pixels along the land–water boundaries, shallow water pixels and water pixels with containing aquatic vegetation are of major concern in the automatic extraction of water pixels. This is due to the fact that the spectral response patterns of these water pixels are similar to that of the noise feature pixels like clouds, cloud shadows, urban settlements, etc. Hence, detailed analysis for each of the sub-groups with varying total brightness levels for identification of the suitable feature parameter and the selection of the threshold value to discriminate water pixels from the noise features is required. NDVI was also used invariably to eliminate non-water pixel, particularly those of vegetation pixels.

The spectral response pattern of the cloud shadow pixels was analyzed to identify the discriminating feature parameter and its threshold values. It is evident from Fig. 5(a) that a combination of NDVI, NIR–green-band ratio with a suitable threshold provides the required discrimination of cloud shadows from water pixels along with a suitable range of brightness values. A similar

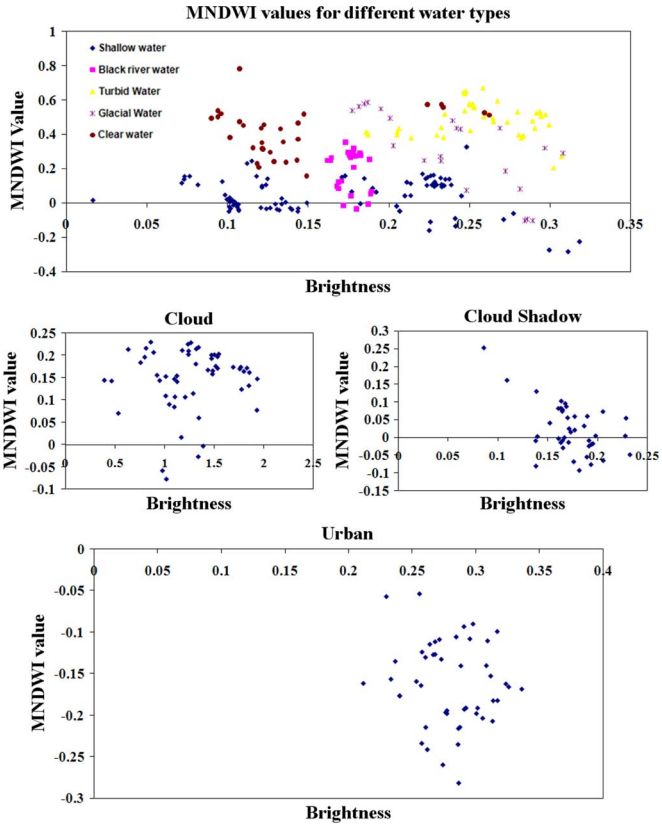

Fig. 7. Scatter plot showing MNDWI values as a function of brightness for various types of water and non-water categories.

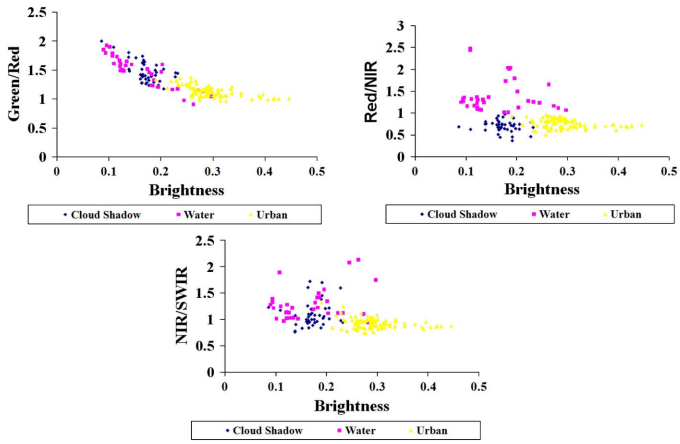

Fig. 8. Scatter plots showing clear water as a function of band ratios.

approach has also been used for discrimination of urban pixels from water pixels.

The type of logics and thresholds implemented for one subcategory of shallow/mixed-water types as an example is given in Table II. The implementation of the logic and threshold is given below.

$$\text{IF } ((\text{Brightness} < 0.2) \text{ AND } (\text{NDVI} < 0.2) \text{ AND } (\text{B2} > 0.9 * \text{B5}) \text{ AND } (\text{B2} > \text{B4})) \text{ THEN } \{\text{shallow water}\} \text{ ELSE } \{\text{check for other types of water}\}. \quad (7)$$

TABLE II
SAMPLE SPECTRAL INFORMATION AND COMPUTATION OF PARAMETERS FOR A TYPE OF SHALLOW WATER PIXELS

Green	Red	NIR	SWIR	Brightness	G/R	G/N	G/S	R/N	R/S	N/S	NDVI	NDWI	MNDWI
0.032715	0.030518	0.03125	0.026855	0.12	1.07	1.05	1.22	0.98	1.14	1.16	0.01	0.02	0.10
0.032471	0.030029	0.031738	0.0271	0.12	1.08	1.02	1.20	0.95	1.11	1.17	0.03	0.01	0.09
0.03418	0.031738	0.032959	0.034668	0.13	1.08	1.04	0.99	0.96	0.92	0.95	0.02	0.02	-0.01
0.03418	0.033203	0.034668	0.033936	0.14	1.03	0.99	1.01	0.96	0.98	1.02	0.02	-0.01	0.00
0.034424	0.033203	0.033203	0.032715	0.13	1.04	1.04	1.05	1.00	1.02	1.02	0.00	0.02	0.03
0.031982	0.029785	0.030273	0.02002	0.11	1.07	1.06	1.60	0.98	1.49	1.51	0.01	0.03	0.23
0.032715	0.029297	0.031982	0.023926	0.11	1.12	1.02	1.37	0.92	1.22	1.34	0.04	0.01	0.16
0.033447	0.031006	0.032227	0.0271	0.12	1.08	1.04	1.23	0.96	1.14	1.19	0.02	0.02	0.11
0.032959	0.030762	0.03125	0.02002	0.12	1.07	1.06	1.65	0.98	1.54	1.56	0.01	0.03	0.24
0.021973	0.014893	0.020264	0.016113	0.07	1.48	1.08	1.36	0.74	0.92	1.26	0.15	0.04	0.15
0.022705	0.014893	0.022217	0.016602	0.08	1.53	1.02	1.37	0.67	0.90	1.34	0.20	0.01	0.16
0.022217	0.014893	0.019043	0.016846	0.07	1.49	1.17	1.32	0.78	0.88	1.13	0.12	0.08	0.14
0.02124	0.014404	0.019043	0.016846	0.07	1.48	1.12	1.26	0.76	0.86	1.13	0.14	0.06	0.12
0.024414	0.018066	0.019287	0.019775	0.08	1.35	1.27	1.24	0.94	0.91	0.98	0.03	0.12	0.11
0.025146	0.024902	0.025391	0.022949	0.10	1.01	0.99	1.10	0.98	1.09	1.11	0.01	-0.01	0.05
0.054932	0.043701	0.044922	0.04126	0.19	1.26	1.22	1.33	0.97	1.06	1.09	0.01	0.10	0.14
0.05249	0.037354	0.042236	0.038818	0.17	1.41	1.24	1.35	0.88	0.96	1.09	0.06	0.11	0.15
Mean value				0.11	1.20	1.06	1.26	0.90	1.07	1.19	0.05	0.03	0.10
Standard deviation				0.03	0.20	0.07	0.19	0.11	0.21	0.18	0.06	-0.06	-0.10
Maximum value				0.14	1.53	1.27	1.65	1.00	1.54	1.56	0.20	0.00	0.00
Minimum value				0.07	1.01	0.99	0.99	0.67	0.87	0.95	0.00	0.06	0.14

TABLE III
SAMPLE SPECTRAL INFORMATION AND COMPUTATION OF PARAMETERS FOR A TYPE OF TURBID WATER PIXELS

Green	Red	NIR	SWIR	Bright	G/R	G/N	G/S	R/N	R/S	N/S	NDVI	NDWI	MNDWI
0.091064	0.105469	0.069336	0.027832	0.29	0.86	1.31	3.27	1.52	3.79	2.49	-0.21	0.13	0.53
0.090332	0.102539	0.070313	0.02832	0.29	0.88	1.29	3.19	1.46	3.62	2.48	-0.19	0.13	0.52
0.091064	0.104004	0.070313	0.028564	0.29	0.88	1.30	3.19	1.48	3.64	2.46	-0.19	0.13	0.52
0.085205	0.089844	0.05957	0.0271	0.26	0.95	1.43	3.14	1.51	3.32	2.20	-0.20	0.18	0.52
0.080322	0.073975	0.054688	0.025635	0.24	1.09	1.47	3.13	1.35	2.89	2.13	-0.14	0.20	0.52
0.091064	0.105957	0.070801	0.029297	0.30	0.86	1.29	3.11	1.50	3.62	2.42	-0.20	0.13	0.51
0.083984	0.087402	0.05957	0.027832	0.26	0.96	1.41	3.02	1.47	3.14	2.14	-0.19	0.17	0.50
0.083984	0.088379	0.063477	0.028564	0.26	0.95	1.32	2.94	1.39	3.09	2.22	-0.16	0.14	0.49
0.077148	0.10791	0.07666	0.027344	0.29	0.72	1.01	2.82	1.41	3.95	2.80	-0.17	0.00	0.48
0.082031	0.098389	0.063477	0.029541	0.27	0.83	1.29	2.78	1.55	3.33	2.15	-0.22	0.13	0.47
0.091553	0.103027	0.070313	0.034424	0.30	0.89	1.30	2.66	1.47	2.99	2.04	-0.19	0.13	0.45
0.09082	0.093018	0.048584	0.032471	0.27	0.98	1.87	2.80	1.92	2.87	1.50	-0.31	0.30	0.47
0.081543	0.085205	0.050537	0.033203	0.25	0.96	1.61	2.46	1.69	2.57	1.52	-0.26	0.24	0.42
0.093506	0.102539	0.057617	0.036865	0.29	0.91	1.62	2.54	1.78	2.78	1.56	-0.28	0.24	0.44
0.097168	0.107422	0.057617	0.032227	0.29	0.91	1.69	3.02	1.86	3.33	1.79	-0.30	0.26	0.50
0.06543	0.073486	0.037842	0.02832	0.21	0.89	1.73	2.31	1.94	2.60	1.34	-0.32	0.27	0.40
0.06665	0.075439	0.037842	0.026367	0.21	0.88	1.76	2.53	1.99	2.86	1.44	-0.33	0.28	0.43
0.06665	0.076416	0.040771	0.030029	0.21	0.87	1.64	2.22	1.87	2.55	1.36	-0.30	0.24	0.38
0.064941	0.075928	0.037354	0.026855	0.21	0.86	1.74	2.42	2.03	2.83	1.39	-0.34	0.27	0.42
0.07251	0.086426	0.045166	0.02832	0.23	0.84	1.61	2.56	1.91	3.05	1.60	-0.31	0.23	0.44
Mean Value				0.26	0.90	1.70	2.54	1.66	3.14	1.95	-0.24	0.19	0.47
Std.deviation				0.04	0.05	0.09	0.24	0.23	0.42	0.46	0.07	0.08	0.05
Max. Value				0.32	0.98	1.87	3.02	2.03	3.95	2.80	-0.15	0.30	0.53
Min. Value				0.20	0.84	1.61	2.22	1.35	2.55	1.34	-0.34	0.00	0.38

Spectral plots [Fig. 3(g) and (h)] for turbid water have different spectral contrast relationships to that of clear water [Fig. 3(a) and (b)]. The typical values of feature parameters for the turbid water pixels and their statistics are shown in Table III. It has been observed that the distinct characteristics of the turbid water pixels are (i) the ratio of reflectance of SWIR and green band is greater than 1.8 and (ii) the reflectance of green band is greater than red band. These values were compared with the values of the non-water pixels and found suitable for extraction of the turbid water pixels. The local implementation takes the form:

$$\begin{aligned}&\text{IF } ((\text{B2} > \text{B3}) \text{ AND } (\text{B2} > 1.8 * \text{B5}))\\&\text{THEN } \{\text{Turbid water}\}\\&\text{ELSE } \{\text{check for other types of turbid water}\}. \qquad (8)\end{aligned}$$

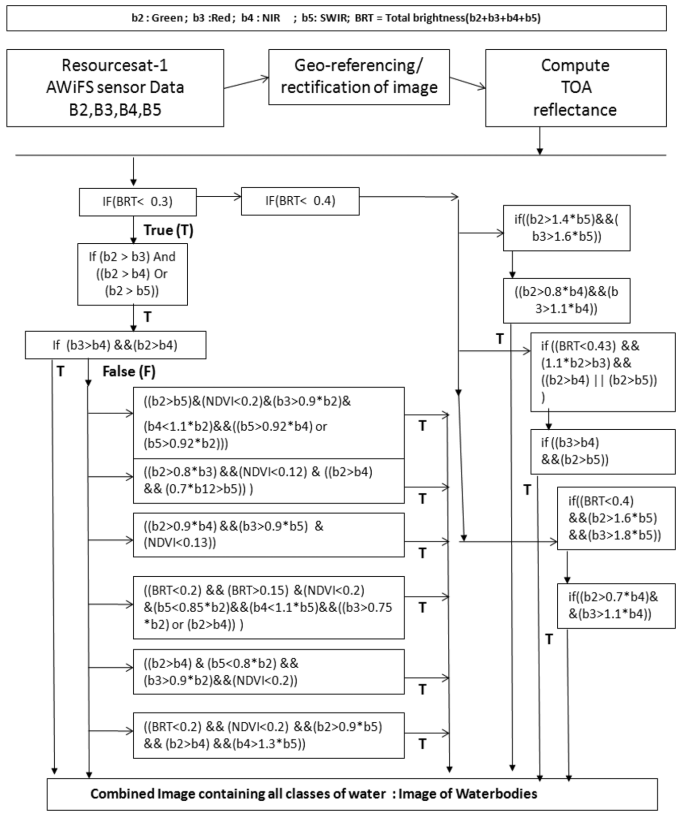

Fig. 9. Flow chart showing the implementation of hierarchical, multi-logic algorithm.

Similar analysis was carried out for each sub-category of water and suitable sets of multi-logical equations were derived. These multi-logic, multi-threshold equations were implemented in a hierarchical manner in Microsoft Visual C++ environment with facilities for the formatted image reading and writing. The logical implementation of the automated water spread mapping algorithm is given in the flow chart in Fig. 9.

IV. TESTING AND EVALUATION OF ALGORITHM

The efficiency of the automatic extraction algorithm for the identification of water pixels from satellite images depends on the detection of water pixels, with desired thematic accuracy. The classification accuracy of water pixels was evaluated by comparing the results of the automatic extraction algorithm with the standard algorithms like MNDWI and NDWI, in which subjective thresholds were applied, unlike the present algorithm. Sample datasets were selected from AWiFS data and the results were obtained by using NDWI, MNDWI and the automatic extraction algorithm. The fraction of pixels identified with each of these methods (Fig. 10) indicates that the automated algorithm provides superior results compared to other standard algorithms like NDWI and MNDWI, particularly in the case of shallow water, mixed land–water boundary pixels by the eliminating pixels due to clouds, cloud shadows and urban settlements. The algorithm was further evaluated with many sub-images containing different types of water bodies, cloud, cloud shadow and urban settlements and the results were found to be satisfactory.

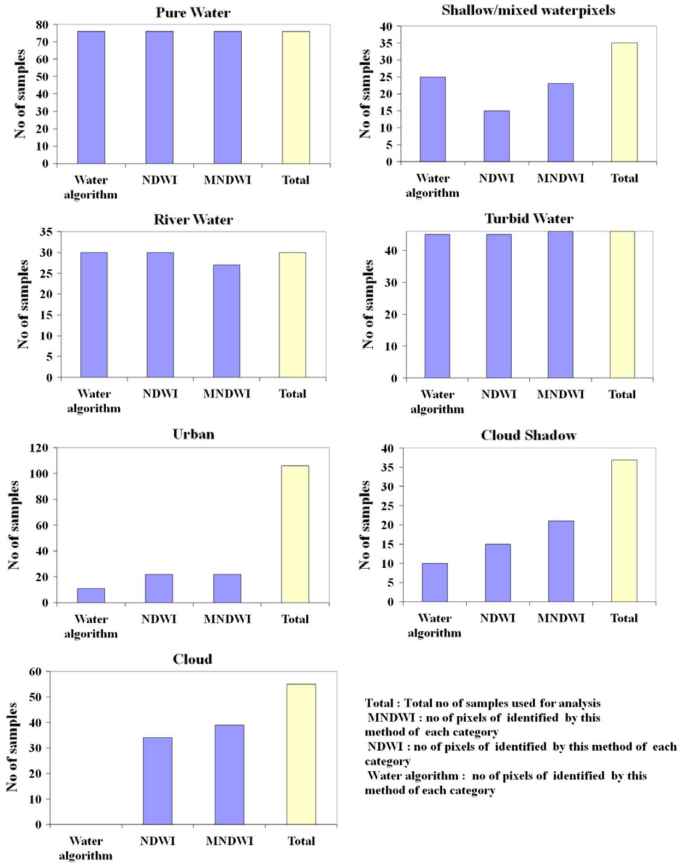

Fig. 10. Comparison of results of hierarchical water algorithm with that of NDWI and MNDWI.

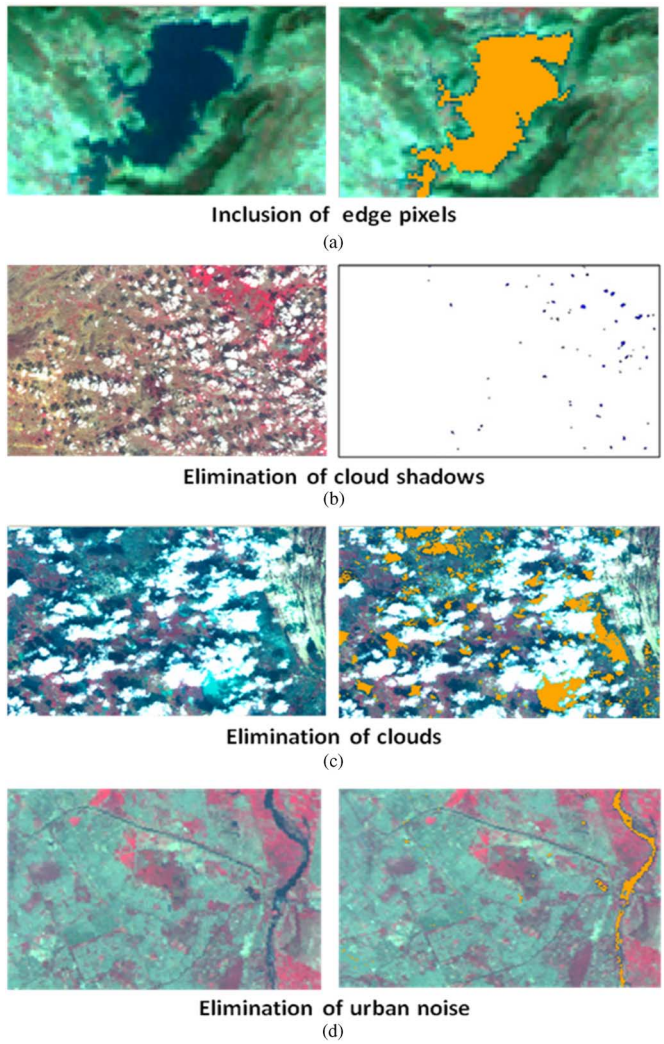

Fig. 11. Illustration showing the elimination of noise and inclusion of edge pixels.

Fig. 11 shows a few typical sample images and the results obtained to illustrate inclusion of edge pixels [Fig. 11(a)] and elimination of cloud shadows [Fig. 11(b)], cloud noise [Fig. 11(c)] and urban settlement noise [Fig. 11(d)].

A comparative study of the automated algorithm *vis-à-vis* the standard algorithm was also carried out for the extraction of the water layer in a scene (Tungabhadra reservoir and its environs, India). The results (Fig. 12) show that the automated feature extraction algorithm is able to eliminate the non-water categories (cloud and cloud shadow pixels) effectively. In the case of the NDWI method, a few cloud shadow pixels were identified as water pixels, while in the case of MNDWI, a few cloud pixels were included in the water pixels. This shows the superiority of the new algorithm.

A. Accuracy Analysis for Water Bodies of Different Shapes and Sizes

Quantitative evaluation of water spread obtained using the algorithm and from visual analysis was carried out with respect to size and shape by comparing the results. Visual interpretation was chosen as it is a well-established technique to capture the land–water boundary, though one or two pixels along the periphery could be ambiguous. Islands within the water bodies are separately identified and their area was excluded while estimating the water spread area (WSA). The accuracy of delineation of water bodies using the automated algorithm *vis-à-vis* visual interpretation has been found to be in the range of 92–97% for large water bodies and varied for the other water bodies depending on the size, area, and area/perimeter. The scatter plot of the accuracy results as a function of area/perimeter is shown in Fig. 13. Lower accuracies were observed for water bodies with smaller area/perimeter containing a higher fraction of boundary pixels.

B. Evaluating the Variations in Temporal Monitoring Using the Algorithm

The change in water volume in a reservoir can be estimated with the change in the WSA and the ground elevation data. Evaluation of the accuracy of the automatic method was carried out by comparing the WSA obtained with the automatic water feature extraction technique with that of hybrid digital–visual interpretation methods for the Tungabhadra reservoir, India, during September–November 2004. Temporal images obtained from the AWiFS sensor over the Tungabhadra reservoir are shown in Fig. 14(a)–(d) along with the results obtained using the automated technique. The WSA estimated with the automatic method along with the values obtained by the hybrid technique for the same image data is given in Table IV. The result shows

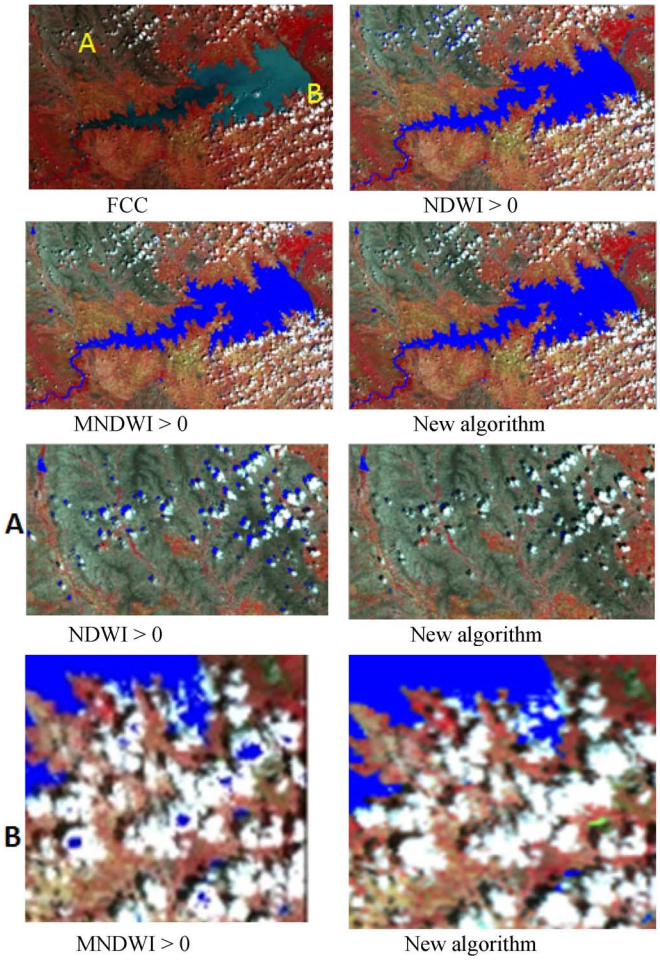

Fig. 12. FCC image of Tungabhadra reservoir and the results obtained with the new algorithm and standard algorithms.

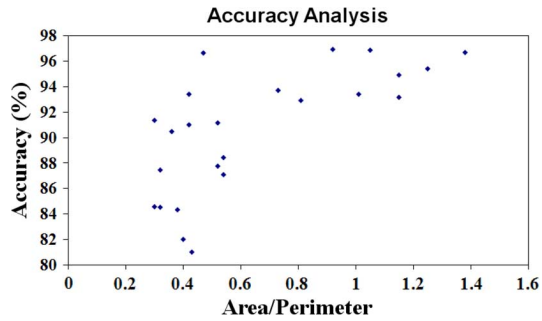

Fig. 13. Scatter plot: Accuracy of water spread area versus area/perimeter.

that the performance of the automatic water feature extraction method is comparable to that of the hybrid digital–visual interpretation technique [5] except for the 03 Sept. 2004 data set. The difference in the magnitude of WSA for the image data acquired on 03 Sept. 2004 [Fig. 14(c)] is due to the fact that the clouds were present in the middle and along the edges of the water body. The above results validate the automatic water feature detection algorithm for temporal change monitoring of WSA and volume of water in a given reservoir

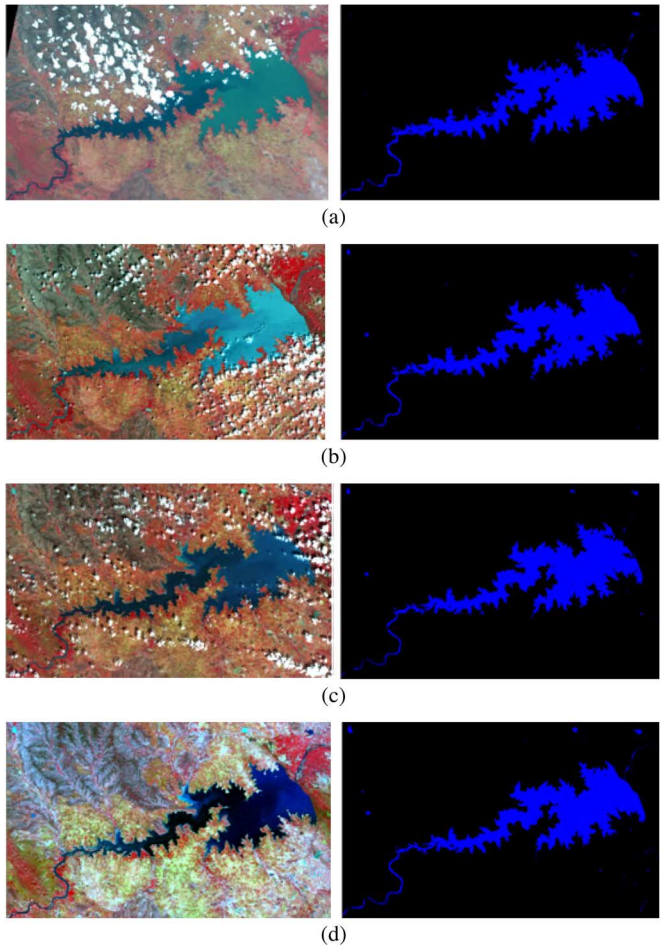

Fig. 14. The temporal monitoring of water spread area estimation using automatic water feature extraction algorithm in the case of Tungabhadra reservoir, Karnataka State. (a) AWiFS imagery acquired on 03 Sept. 2004 and water; (b) AWiFS imagery acquired on 01 Oct. 2004 and water; (c) AWiFS imagery acquired on 25 Oct. 2004 and water; (d) AWiFS imagery acquired on 04 Nov. 2004 and water.

TABLE IV
TEMPORAL CHANGE MONITORING OF WSA AND VOLUME OF WATER IN TUNGABHADRA RESERVOIR DURING SEPTEMBER–NOVEMBER 2004

Date of Satellite over pass	Reservoir Water Elevation (m)	Water spread Area (M. Sq. m)		Difference In Elevation (m)	Capacity between Elevations (M.cu.m)	
		Hybrid analysis	Automatic algorithm		Hybrid analysis	Automatic algorithm
04th Nov. 2004	495.61	300.18	301.00			
				0.7346	228.0219	228.908
25th Oct. 2004	496.35	320.74	322.34			
				0.7712	256.6662	255.8036
01st Oct. 2004	497.12	345.04	341.14			
				0.6187	217.6834	209.7255*
03rd Sept. 2004	497.74	358.69	336.82			

*Reduction in volume is underestimated due to the presence of cloud within the boundary of water body.

V. RESULTS AND DISCUSSION

Both the qualitative/visual inspection and quantitative analysis of the results shows that the new algorithm is suitable for the extraction of water body information from AWiFS satellite data at regular intervals for monitoring the availability of water at regional, state or country level. It can also be used to

TABLE V
COMPARISON OF BANDWIDTHS IN DIFFERENT SATELLITE SENSORS IN VISIBLE AND SHORT-WAVE INFRARED REGIONS

Satellite/ Sensor	Band width	Lmax	Lmin	DN max	Spatial Resolution	Radiometric Resolution
	µm	W/m2-Sr-micron	W/m2-Sr-micron		m	(W/m2-Sr-micron)/Unit DN Value
Resourcesat -1 AWiFS						
B2	0.52 - 0.59	52.34	0	1024	56	0.051113281
B3	0.62 - 0.68	40.75	0	1024	56	0.039794922
B4	0.76 - 0.86	28.425	0	1024	56	0.027758789
B5	1.55 - 1.7	4.645	0	1024	56	0.004536133
Resourcesat -1 LISS III						
B2	0.52 - 0.59	12.064	0	128	23.5	0.094250000
B3	0.62 - 0.68	15.131	0	128	23.5	0.118210938
B4	0.76 - 0.86	15.757	0	128	23.5	0.123105630
B5	1.55 - 1.7	3.397	0	128	23.5	0.026539063
Landsat ETM						
B2	0.52-0.60	30.09	-0.64	256	30	0.120039063
B3	0.63-0.69	23.44	-0.05	256	30	0.096171875
B4	0.76-0.90	24.11	-0.51	256	30	0.096171875
B5	1.55-1.75	3.106	-0.1	256	30	0.012523438
ASTER						
B1	0.52 - 0.60	170.80	0	253	15	0.675098814
B2	0.63 - 0.69	179.00	0	253	15	0.707509881
B3	0.76 - 0.86	106.80	0	253	15	0.422134387
B4	1.60 - 1.70	55.00	0	253	30	0.217391304

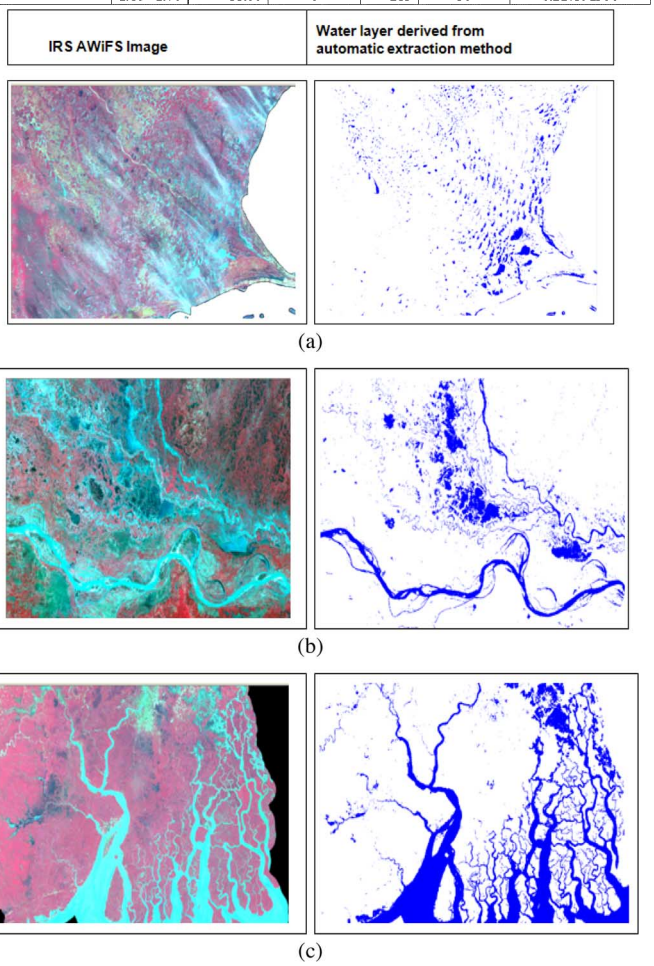

Fig. 15. Typical sub-images and the mapping of the water bodies using automated algorithm. (a) Cascade of small and medium irrigation tanks in Ramanathapuram district, Tamilnadu State; (b) river meandering and moist areas of Indogangetic plains, Bihar state; (c) river with varying levels of turbidity, coastal West Bengal State.

automatically alert when the water spread goes below critical or pre-specified limit(s) for planning suitable water management strategies.

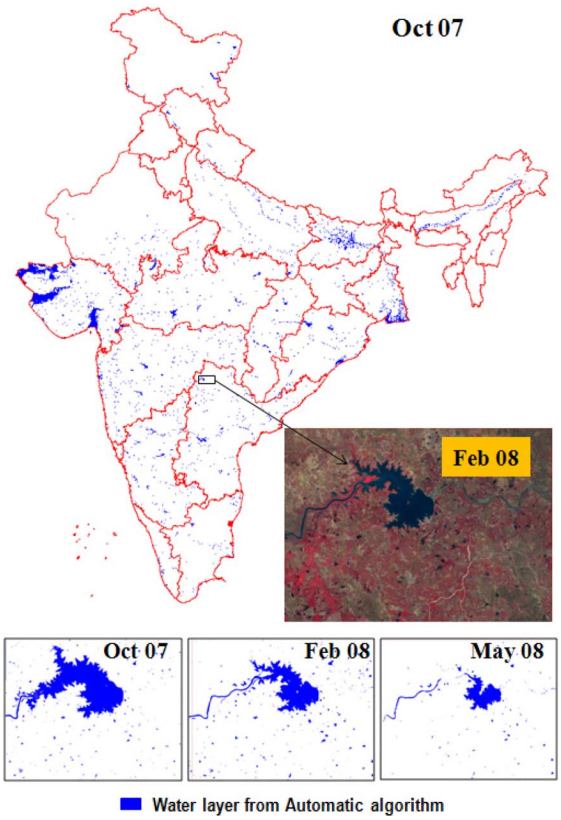

Fig. 16. Spatio-temporal information on water bodies derived from automatic extraction algorithm during October 2007.

Closer examination of the results indicate that automatic extraction algorithms can identify maximum number of water bodies clearly, including the smaller tanks of >10 ha and also eliminate cloud, cloud shadows, and urban settlement noise in water extraction. Evaluation tests were also conducted with images (state-level mosaics) obtained from various regions that contained water bodies of different sizes and shapes. Fig. 15 shows a few typical sub-images and the results obtained using the automated algorithm in different environments and seasons. These results show the efficiency of the algorithm to provide satisfactory results in different geological environments and different seasons of the year. The algorithm was implemented on India mosaic images (60000×60000 pixels) acquired during kharif, rabi and summer seasons of the crop year, and a view of kharif 2007 is shown in Fig. 16. The visual inspection and evaluation of the water bodies mapping results at 1:250000 scale has shown the robustness of the automatic water feature extraction algorithm for monitoring water bodies of various sizes and in different seasons. Satellite-derived intra/inter-seasonal water spread information has been used for dissemination to the public through the web portal Bhoosampada (www.nrsc.gov.in).

Since the automated water extraction algorithm was developed essentially based on the spectral contrast of features, an attempt was made to evaluate the same with the data obtained from other sensors having similar spectral bands such as ResourceSat-1 LISS III, LANDSAT ETM and ASTER. However, it must be noted that though the spectral bands are similar, their

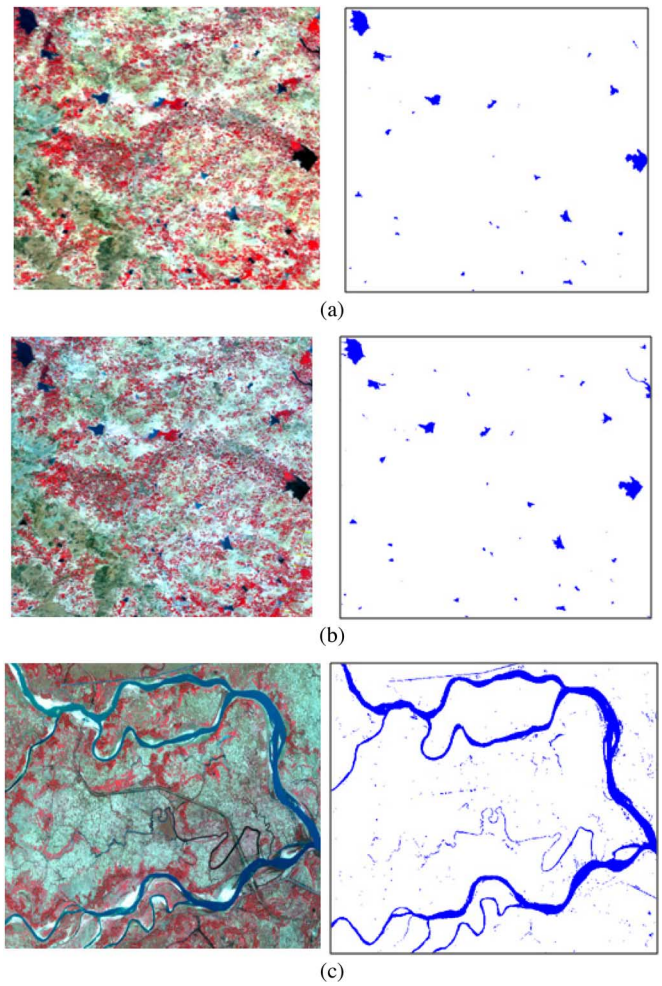

Fig. 17. Water layer extracted using automated extraction algorithm for IRSLISSIII, ASTER, Landsat-ETM sensors. (a) AWiFS data acquired on 03 July 2009 and water layer; (b) LANDSAT ETM data acquired on 03 Sept. 2009 and water layer; (c) ASTER data acquired on 02 Aug. 2006 and water layer.

radiometric resolutions are quite different (Table IV). The algorithm was evaluated with the data obtained for the same study area acquired from Landsat TM (03 Sept. 2009), IRS AWiFS (03 July 2009) and the results are shown in Fig. 17(a) and (b). The results from ASTER data (06 Aug. 2006) is also shown in Fig. 17(c). The results show that the algorithm is suitable for these datasets as well. Similarly, ResourceSat-1 LISS III data and AWiFS data acquired on the same day (27 Feb. 2006) were used in the algorithm for water extraction which has provided a comparable result [Fig. 18(a) and (b)]. The algorithm is sensitive to spatial resolution; few of the water bodies identified using LISS III sensor data were not identified in AWiFS data due to its coarser spatial resolution. When national datasets of IRS LISS III were evaluated, it was found that a few pixels corresponding to highly turbid water bodies were not detected due to the lower radiometric resolution and dynamic range. Hence, the required minor modifications for spectral thresholds were implemented to obtain satisfactory results. A similar exercise would improve the efficiency of the algorithm to enable the national/global application of the algorithm for other sensors having similar spectral bands.

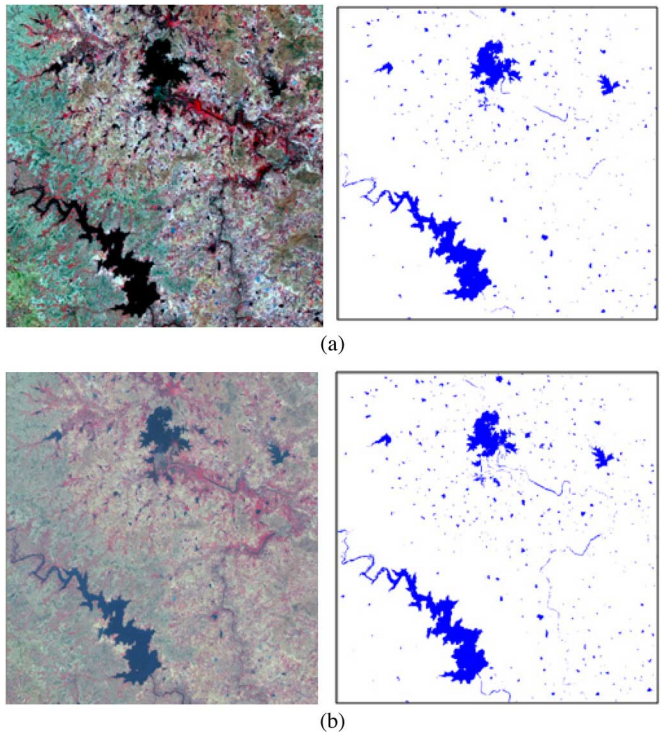

Fig. 18. Water layer extracted using automated algorithm from concurrent IRS AWiFS, LISS III data for the study area. (a) IRS AWiFS data acquired 27 Feb. 2006 and water layer; (b) IRS LISS III data acquired on 27 Feb. 2006 and water layer.

VI. Conclusion

Spatio-temporal information across inter/intra-seasonal variation in surface water bodies is a valuable tool for better water resources planning and management. With the advent of spatial information technologies, namely Remote sensing and GIS, a number of satellite missions are providing the synoptic coverage of larger areas with high repetivity to generate spatio-temporal information on water bodies. In view of the existing limitations in image classification methods for quick extraction of water bodies, an algorithm to automatically extract water pixels from satellite image has been developed for IRS AWiFS sensor data. The methodology presented in this study was implemented on a large number of datasets of India after validation. The evaluation of the algorithm with other sensor data such as ResourceSat-1 LISS III, Landsat ETM, and ASTER showed satisfactory results. However, minor modifications may be required for application of the algorithm for global/national scale implementation to account for the lower radiometric resolution of these sensors.

The spatio-temporal information on water spread area was derived using the automatic extraction algorithm for India during May 2004, June 2005, July 2006 and Aug. 2007 representing the crop seasons (kharif, rabi, and summer). The technique developed here can be applied for inventory for creation/updating of databases on water bodies, enabling the development of the Water Bodies Information System at national/global scales. Further, this information would also be useful for disaster management support systems dealing with drought and flood databases and in studies related to the effect of climate change. The results (spatio-temporal

maps) are published on the web site Bhoosampada of NRSC (www.nrsc.gov.in). The results of the present study are useful to enable the development of web-based water bodies information generation and dissemination system in near-real-time mode.

ACKNOWLEDGMENT

The authors thank the director of NRSC for encouraging the research on the topic and providing full support. The authors are also grateful to the Group Directors of the Land Resources Group and Water Resources Group and the head of the Water Resources Division at NRSC for their valuable suggestions.

REFERENCES

[1] F. F. Sabins, *Remote Sensing: Principles and Interpretation*, 3rd ed. New York: W. H. Freeman and Company, 1997.

[2] C. Rafael, Gonzalez, and R. E. Woods, *Digital Image Processing*, 2nd ed. Englewood Cliffs, NJ: Prentice-Hall, 2002.

[3] P. S. Frazier and K. J. Page, "Water body detection and delineation with landsat TM data," *Photogramm. Eng. Remote Sens.*, vol. 66, pp. 1461–1468, 2000.

[4] P. Manavalan, P. Sathyanath, and G. L. Rajegowda, "Digital image analysis techniques to estimate water spread for capacity evaluations of reservoirs," *Photogramm. Eng. Remote Sens.*, vol. 59, pp. 1389–1395, 1993.

[5] A. V. Suresh Babu, M. Shanker, V. V. Rao, and V. Bhanumurthy, "Generation of water spread contours for Tungabhadra reservoir during low water levels of the year 2002 using satellite remote sensing technique," in *Proc. GIS India 2003*, Jaipur, India, 2003.

[6] B. S. D. Sagar, M. Venu, and B. S. P. Rao, "Distributions of surface water bodies," *Int. J. Remote Sens.*, vol. 16, pp. 3059–3067, 1995.

[7] A. V. Kulkarni, S. K. Singh, P. Mathur, and V. D. Mishra, "Algorithm to monitor snow cover using AWiFS data of ResourceSat-1 for the Himalayan region," *Int. J. Remote Sens.*, vol. 27, pp. 2449–2457, 2006.

[8] A. V. Suresh Babu, P. Roy, and S. Subramaniam, "Automatic extraction of waterbodies from IRS AWiFS data," *Int. J. Geoinform.*, vol. 3, no. 3, pp. 63–71, 2007.

[9] S. K. McFeeters, "The use of normalized difference water index (NDWI) in the delineation of open water features," *Int. J. Remote Sens.*, vol. 17, pp. 1425–1432, 1996.

[10] B. L. Markham and I. J. Barker, "Landsat MSS and TM post-calibration dynamic ranges, exoatmospheric reflectances and at-satellite temperatures," *EOSAT Technical Notes*, vol. 1, pp. 3–8, 1986.

[11] A. S. KiranKumar, "Advanced Wide Field Sensor (AWiFS)," *SAC Courier*, vol. 28, pp. 3–7, 2003.

[12] H. Xu, "Modification of normalize difference water index (NDWI) to enhance open water features in remotely sensed imagery," *Int. J. Remote Sens.*, vol. 27, pp. 3025–3033, 2006.

[13] M. Islam and K. Sado, "Analyses of ASTER and Spectroradiometer data with *in situ* measurements for turbidity and transparency study of lake Abashr," *Int. J. Geoinform.*, vol. 2, pp. 31–45, 2006.

[14] Y. H. Ahn, P. Shunmugam, and J. H. Ryu, "Atmospheric correction of the Landsat satellite imagery for turbid waters," *GAYANA*, vol. 68, no. 2, pp. 1–8, 2004, supl. TIProc Concepción .

S. Subramaniam received the Bachelor of Science in 1974 and the Master of Science in 1976 in physics from Madurai University, India.

After working in industry for two years, he joined the National Remote Sensing Agency, Hyderabad, India, in 1979. He was engaged in research in the areas of optical and electro-optical instrumentation and optical image processing until 2004. His current areas of research are digital image analysis techniques for automation and image processing for remote sensing data. He is a fellow of the Optical Society of India and a life member of the Indian Society of Remote Sensing, Indian Physics Association, and Indian Aerosol Science and Technology Association.

A. V. Suresh Babu received the Bachelor degree in 1995 and the Master degree in 1997 in agricultural engineering, and the Ph.D. degree in water resources in 2007.

He has been working in RS and GIS applications domain, specifically in water resources, since 1998, and has expertise in utilization of spatial information technologies for demonstrating the space inputs for real-time applications in planning irrigation systems, high-resolution satellite data applications for irrigation infrastructure mapping and monitoring, benchmarking studies of irrigation systems/command area monitoring, reservoir sedimentation studies, and agricultural drought assessment. He has been working to make use of nationwide temporal satellite datasets for quick generation and analysis of seasonal water spread.

Partha Sarathi Roy during his thirty-three year scientific career has made original contributions to the development of satellite remote-sensing-based methodologies for vegetation cover type discrimination using phenology as discriminant function and biodiversity characterization using landscape ecological parameters. He has made pioneering contribution to estimate biomass and NPP of forests using homogenous vegetation strata (HVS) and spectral modeling techniques from earth observation platforms. He has been on the international team to develop semi-expert systems for forest cover density mapping with ITTO, Japan, Global Land Cover 2000 mapping (an initiative undertaken in Millennium Ecosystem Program of UN-FAO and ESA) and validation for South-Central Asia (ISPARA Italy). He has developed remote-sensing-based methods for forest biomass and NPP estimation. Presently, he is studying LULC dynamics and its impact on bio-geochemical and hydrological cycles in Indian River basins in the context of human dimensions of climate change.